ELSEVIER

Polymer 42 (2001) 6187–6198

polymer

www.elsevier.nl/locate/polymer

Viscoelastic behaviour and time–temperature correspondence of HDPE with varying levels of process-induced orientation

J.F. Mano[a,*], R.A. Sousa[a,b], R.L. Reis[a], A.M. Cunha[a], M.J. Bevis[b]

[a]*Department of Polymer Engineering, University of Minho, Azurém Campus, 4800-058 Guimarães, Portugal*
[b]*Wolfson Centre for Materials Processing, Brunel University, Uxbridge, Middlesex UB8 3PH, UK*

Received 12 October 2000; received in revised form 26 January 2001; accepted 26 January 2001

Abstract

Shear controlled orientation in injection moulding (SCORIM) is a non-conventional injection moulding technique that allows for the enhancement of the mechanical properties of semi-crystalline polymers. In this work the flexural mechanical feature, namely their time-dependence, of conventionally injection-moulded high-density polyethylene (HDPE) (PEc) and SCORIM-processed HDPE (PEs) are compared. The differences should be attributed to the appearance of highly oriented structures such as shish-kebab morphologies in the latter case. The quasi-static performance of HDPE shows a 59% increase in the flexural modulus following SCORIM application. Master curves of the frequency-dependence of the storage modulus and of the time-dependence of strain were constructed successfully in the region of the α-relaxation. The viscoelastic data are well described by the Cole–Cole model. The wide broadness of the distribution of relaxation time observed for both materials is ascribed to the molecular mobility of the amorphous phase involved in the relaxation process. Two approaches were used to investigate the curvature observed in the Arrhenius plots. In the first case, two separate processes were assumed to contribute to the α-relaxation, with activation energies of 150–170 and 180–210 kJ mol^{-1}, respectively (dynamic data). However, the two α-processes, αI and αII, often reported in the literature, did not appear explicitly in the original data, which showed a single peak in an E'' vs T plot. Therefore, a unique process for the α-relaxation was also assumed and was well described taking into account changes in the reduced volume whose temperature-dependence obeys a general equation of state. This concept enabled a good agreement between creep and dynamic experiments.

Keywords: Polyethylene; Orientation; Relaxation

1. Introduction

The quest for polymeric materials with high mechanical performance has resulted in several complementary approaches. The synthesis of new materials and the chemical (for example, grafting, branching or cross-linking) and/or physical (for example, blending, compounding or annealing) modification of existing polymeric materials are used for the development of polymers with enhanced mechanical properties. Other attempts rely on structure manipulation during melt processing. In fact, the control of the thermomechanical conditions imposed upon the polymer provides for considerable enhancement of the anisotropy of the polymer with positive cost and engineering implications. The solid state engineering processes such as tensile drawing [1,2], die drawing [3] and hydrostatic extrusion [4,5] of polyethylene (PE) are examples where the application of this principle to a semi-crystalline thermoplastic material is highly effective.

It is also possible to confer a strong anisotropic behaviour to injection-moulded PE by means of processing techniques such as high-pressure injection moulding [6] and shear-controlled orientation in injection moulding (SCORIM) [7–11]. The former technology is based on the combined application of very high pressures and special mould designs [6]. By contrast, the SCORIM technology relies on the application of shear stress fields to the melt/solid interfaces during the packing stage by means of hydraulically actuated pistons [9]. After the filling of the cavity mould, the molten polymer is continuously sheared as the solidification progressively occurs from the mould wall to the moulding core part. As a result of SCORIM processing, a highly sheared crystalline phase of PE can be obtained, exhibiting a significant improvement of mechanical performance [7,8]. The microstructure texture and the molecular orientation level developed under processing also determine the time-response for a given mechanical excitation. In fact,

* Corresponding author. Tel.: +351-5360-4451; fax: +351-2535-10249.
E-mail address: jmano@dep.uminho.pt (J.F. Mano).

0032-3861/01/$ - see front matter
PII: S0032-3861(01)00090-8

the consequent chain mobility within the material depends on the anisotropic character induced during processing.

Although the microstructure and the tensile quasi-static mechanical properties of PE were processed by both conventional and SCORIM routes were already described [8], the time-dependent mechanical performance of such materials has never been reported. Such investigation allows for a better understanding of the viscoelastic properties that may be useful for design purposes and for predicting the very short or long time behaviour of the moulded parts.

The general relaxation processes in semi-crystalline polymeric systems have been investigated in detail [12,13]. The most practically important of these investigations is that of the drop in stiffness that takes place in certain regions of temperature, each one associated with an anelastic relaxation process. In a more general case, the time-response of these materials upon any kind of mechanical or electric stimulus may depend strongly on the fact that some relaxational process can occur at these temperature/time scales. There is also a need for associating the observable relaxations with the description of the molecular processes underlying them.

In PE at least three relaxational processes can be observed, labelled as γ, β and α, from low to high temperatures [12,13]. The γ-process has been assigned to the so-called crankshaft mechanisms in the amorphous phase [13] whereas the β-relaxation corresponds to the glass transition of PE [12–15]. In this work we focus on the study of the α-relaxation, which corresponds to a complex process involving molecular mobility within the crystalline phase. In fact, the largest changes in the mechanical properties of polyethylenes with moderate to high crystallinities are caused by the α-process. This relaxation also takes place above room temperature where, in many cases, the material is being used. Moreover, as mentioned in Ref. [16], the α-relaxation is related to important material properties such as creep, annealing, crystallisation, extrudability and drawability.

The mechanical response of the α-process in HDPE is very different from that in low-density PE (LDPE) and some authors claim that it consists, in fact, of two or more relaxation mechanisms [17]. The two processes were designated αI, αII by Nakayasu et al. [18] and α, α' by McCrum and Morris [19]. Several studies have been carried out in order to assign these processes to specific types of changes at the molecular level (see, for example, Refs. [12,13,16,20–29]). The αI-, or α-, process, which will be discussed throughout this paper in much more detail, has been associated with 180° chain flips within the crystalline regions. The αII-, or α'-, process should be related, according to Takayanagi, to the molecular motions parallel to the chain axis in the crystalline phase as the crystals thicken during the recrystallisation that occurs in the region above 80°C [27]. Iwayanagi proposed that the αII-relaxation is a boundary phenomenon analogous to grain boundary slip observed in metals [28,29].

The kinetics of such relaxations has been often quantified in terms of its activation energy. The αI-, or α-, process shows activation energies around 117 kJ mol^{-1} when studied by mechanical techniques [18] and 120 kJ mol^{-1} [12] in dielectric measurements. The αII-, or α'-, process occurs at higher temperatures, with activation energy around 201 kJ mol^{-1} [20] and is not observed by dielectric measurements.

The concept of the activation energy was furthered by Glasstone et al. in the 1930s and presented in detail in their 1941 book [30]. It is based on a century-old work by Svante Arrhenius. We shall also investigate this concept in the present paper.

2. Materials and methods

The material studied here was a high-density polyethylene (HDPE), grade HD8621, from DSM (The Netherlands) with a melt flow index (MFI) of 0.16 g/10 min, a number average molecular weight ($\langle M_n \rangle$) of 7000 and a weight average molecular weight ($\langle M_w \rangle$) of 2.1×10^5, which gives the polydispersity index ($\langle M_w \rangle / \langle M_n \rangle$) of 29.

Both conventional, PEc, and shear-controlled orientation injection moulding (SCORIM), PEs, samples were produced in a Demag D-150 NCIII-K conventional moulding machine fitted with a SCORIM device. Axysymmetric tensile test bars with 5 mm diameter were moulded using optimised conditions [8]. A schematic diagram of a SCORIM head is shown in Fig. 1 together with the periodic variation of the hydraulic pressure of the SCORIM pistons for its possible modes of operation. Mode A is characterised by the out-of-phase oscillation of the pistons, which causes the shear of the melt inside the mould. Mode B corresponds to the in-phase oscillation of the pistons. This mode of operation causes successive compression and decompression of the melt. Finally, in mode C, both pistons are held down at a constant pressure, promoting the packing of the melt inside the mould. The more relevant processing parameters during the SCORIM cycle are [8]: the frequency and pressure of piston oscillation, the time for each SCORIM stage and the holding pressure level defined by the injection moulding machine. Each SCORIM cycle is defined by a suitable number of independent stages. For each one, it is possible to combine several modes and conditions of operation. The samples studied in this work were processed by a combination of two shear stages (mode A operation) and a final packing stage (mode C operation) [8]. It was shown previously [8], that the optimisation of SCORIM conditions should consider the interdependence of the processing parameters. Further information on the processing conditions and structural development in SCORIM mouldings can be found in Refs. [7,8].

Flexural tests were performed on an Instron 4505 tensile testing machine in a controlled environment (23°C and 55% relative humidity). Flexural tests were performed at 5 mm min^{-1} (8.33×10^{-5} m s^{-1}) following a three-point

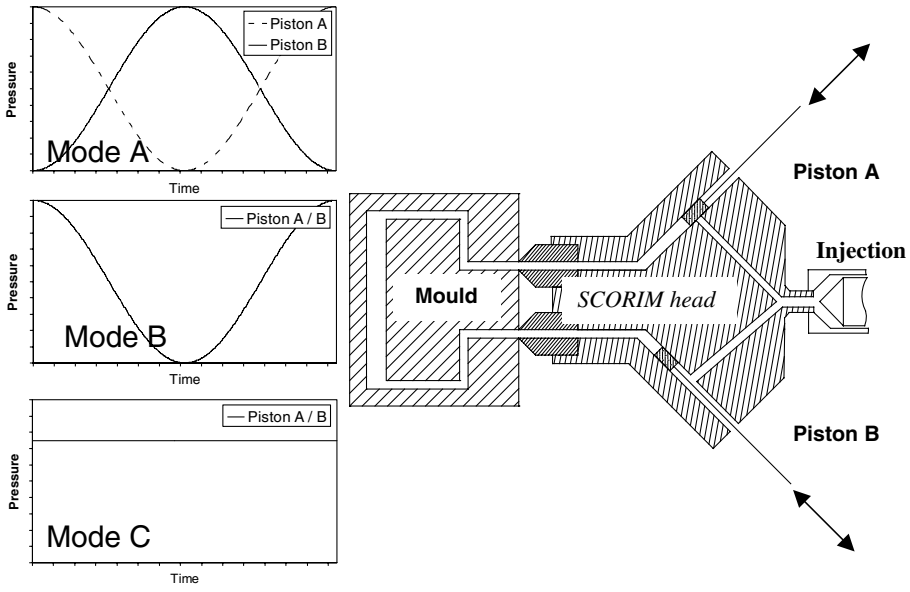

Fig. 1. Schematic diagram of a SCORIM device and the respective modes of operation in terms of the hydraulic pressure variation in the pistons A and B: mode A — out-of-phase oscillation of the pistons with the consequent shear of the melt inside the mould; mode B — in-phase oscillation of the pistons, causing the compression and decompression of the melt inside the mould; and mode C — compression of the pistons at a constant pressure, which promotes the packing of the melt inside the mould (adapted from Ref. [9]).

bending loading scheme (30 mm span), using samples with 35 mm length (machined from the moulded specimens), in order to determine the flexural modulus (secant modulus at 0.8% strain — $E_{0.8\%}$) and the maximum flexural stress (σ_m) — flexural strength.

Microtome cut cross-sections of the mouldings were observed by polarised light microscopy (PLM) in an Olympus microscope. Scanning electron microscopy was used for fractographic analysis and was carried out on selected sets on a Leica Cambridge scanning electron microscope. All the surfaces were mounted on a copper stub and coated with Au + Pd alloy prior to the examination.

The dynamic mechanical apparatus used in this work was a DMA7e Perkin–Elmer analyser with a controlled cooling accessory. Continuous flux of high-purity helium (flow rate of $\sim 28\ cm^3\ min^{-1}$) was used to improve heat transfer throughout the sample surroundings during the experiments. The experiments were carried out in the three-point bending mode. The samples were obtained by cutting the extremities of the injection-moulded pieces in order to obtain cylindrical bars with 23 mm length. The samples were placed over a 20-mm bending platform and a 5-mm knife-edge probe tip provided the mechanical excitation. For all the isothermal dynamic experiments a static stress of 1.2×10^5 Pa and a dynamic stress of 1.0×10^5 Pa were imposed on the sample. The frequency range used was 0.5–30 Hz and the studies were carried out in the temperature range 0–95°C.

Creep experiments were also performed in the DMA7e Perkin–Elmer apparatus according to the same loading scheme. The static stress imposed was 1.0×10^5 Pa. The experiments were carried out at different temperatures, between −40 and 100°C.

3. Fracture surfaces

Figs. 2 and 3 show for PEc and PEs samples, respectively, cryogenic fracture surfaces and polarised light microscopy (PLM) photographs for both mouldings. The conventional injection mouldings exhibit a skin and a large spherulitic core (Fig. 2). The frozen skin corresponds to a rapidly cooled region, where the molecular orientation induced by the shear stress field imposed on the melt during flow is frozen in. This morphological development gives rise to a smooth texture.

Within the range of thermomechanical conditions that can be imposed in conventional injection moulding the thickness of the skin is always limited. This can be overcome by using a technique such as SCORIM, which allows for the generation of additional oriented layers. In fact, the strong anisotropic character of PEs is evident from the observation of the fracture surface and from the layered morphology observable by optical microscopy. The orientation rings are clear in Fig. 3, being typical of the out-of-phase operation of the SCORIM equipment These consecutive layers, solidified under a controlled macroscopic shear, are mainly responsible for the enhanced mechanical performance of SCORIM-moulded samples.

In the PLM photographs shown in Fig. 3 it is possible to identify three types of microstructures: (i) a skin with the same texture and origin as in conventional mouldings (compare to Fig. 2); (ii) a zone of highly oriented layers; and (iii) a spherulitic core (compare to Fig. 2). These oriented layers were induced by the shear stress field imposed during the oscillating packing stage, at the melt/solid interface, but they were cooled down at a slower rate

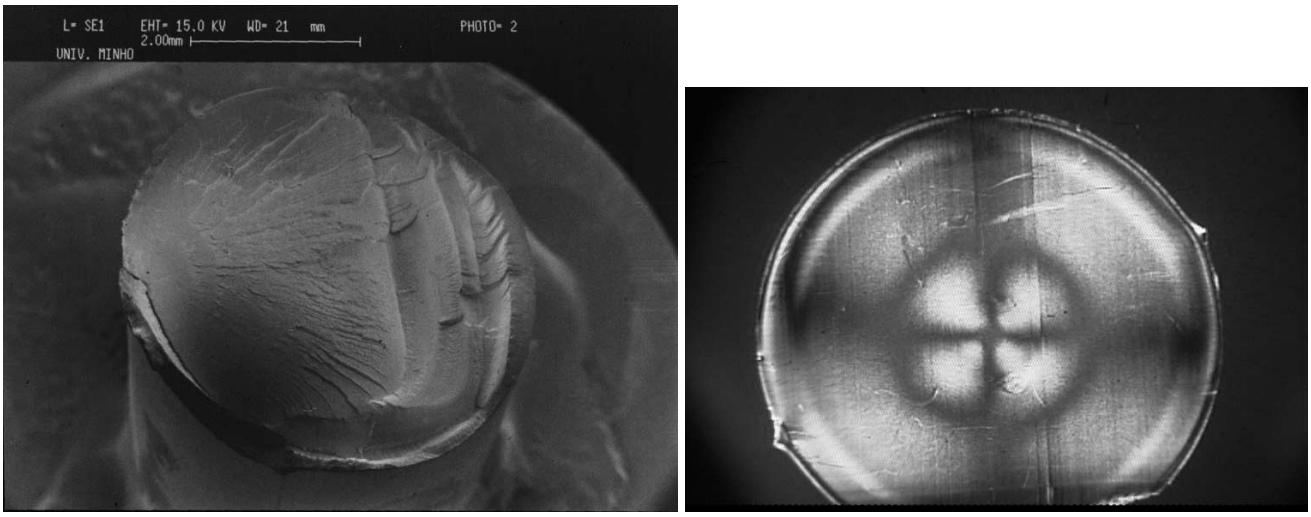

Fig. 2. SEM micrograph of a fracture surface and polarised light microscopy of PEc samples (diameter of the studied samples: 5 mm).

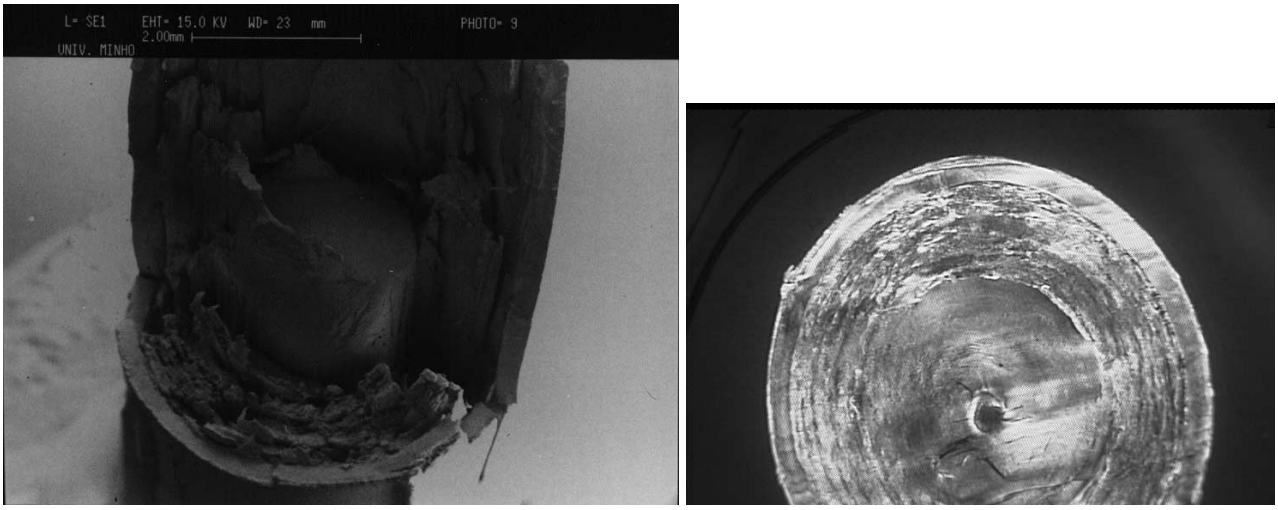

Fig. 3. SEM micrograph of a fracture surface and polarised light microscopy of PEc samples (diameter of the studied samples: 5 mm).

than the skin material due to the insulating effect of the previously solidified polymer. The thickness and orientation of these layers depends on the processing history. During the SCORIM shear stage, the extension and orientation of the macromolecules is high at the melt/solid interface; this raises the melting point, T_m, increases the amount of supercooling for a given $T < T_m$ and enhances the driving force for crystallisation under a stressed state. In the case of PE the crystallisation of the extended macromolecules gives rise to a characteristic X-ray diffraction [8] from which the presence of the *c*-axis-crystallised fibres may be deduced. The unstretched portions of extended PE chains crystallise in the form of chain-folded lamellae [31], which in combination with the fibres previously crystallised, form a so-called shish-kebab structure [31]. However, the degree of anisotropy in moulded components that results from the

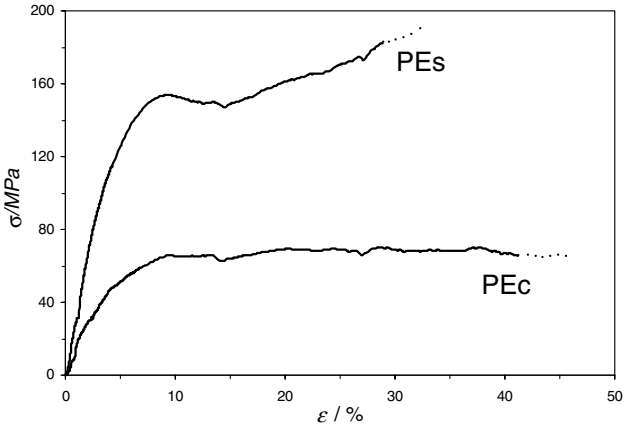

Fig. 4. Stress/strain curve of both conventional (PEc) and SCORIM (PEs) processed HDPE (flexural experiments).

Table 1
Flexural test results for conventional (PEc)and SCORIM (PEs) mouldings. The tensile modulus, based on calculations with data reported in a previous work [8] is also included

	Flexural		Tensile $E_{0.8\%}$ (GPa) [8]
	$E_{0.8\%}$ (GPa)	σ_m (MPa)	
Pec	2.2 ± 0.3	72 ± 4	1.1
PEs	3.5 ± 0.5	183 ± 4	5.8

existence of shish-kebab structures is believed to vary along the cross-section. The layered cross-section morphology shown for SCORIM-processed HDPE in Fig. 3 reveals different thermomechanical histories across the thickness. The continuous crystallisation of the polymer, from the mould wall to the core, is driven by the cooling process resulting from the heat removal by thermal conduction, being favoured by the orientation state of the macromolecules that induces the nucleation process. After crystallisation, a structure gradient is expected in SCORIM-processed HDPE. The morphology of the obtained mouldings develops from a high density of row structures with small lamellae (the shish-kebabs) in the vicinity of the mould wall to a spherulitic core as a result of the negligible stress field in the central part.

4. Quasi-static mechanical results

The flexural stress vs strain curves for PEc and PEs are presented in Fig. 4. In both cases, the final strain was defined by the maximum displacement possible with the loading device employed (~40%) and not by the failure of the sample. Table 1 presents the flexural testing results for both PEc and PEs, together with the corresponding tensile modulus as presented in a previous work [8]. To our knowledge such kinds of result were never reported. PEc has flexural modulus equal to 2.2 GPa and flexural strength equal to 72 MPa. When moulded by the SCORIM procedure, PE exhibits 3.5 GPa and 183 MPa of flexural strength, accounting for increases of stiffness and strength of 59 and 154%, respectively. However, the improvement of stiffness achieved with SCORIM in the flexural mode is less than that reported for the tensile testing [8].

5. Dynamic mechanical results

HDPE exhibits a strong non-linear behaviour even at low stress levels [32,33]. An efficient method to isolate experimentally the linear viscoelastic contribution is based on the application of a dynamic stress excitation at low strain levels. In these conditions the dynamic strain signal will not be influenced by an irrecoverable deformation process since, even at high temperatures, the development of irrecoverable strain during a dynamic cycle is negligible.

The dynamic mechanical results are expressed usually as the complex modulus, $E^* = E' + iE''$ (E' and E'' are the storage and loss moduli), the complex compliance, $D^* = D' - iD''$ and the loss factor, $\tan\delta = E''/E' = D''/D'$. The complex modulus and compliance are related by $E^* = 1/D^*$. Mechanical dynamic studies on SCORIM samples were never reported before. In the present study the dynamic results for PEc and PEs are summarised in Fig. 5 in terms of the frequency-dependence of the storage modulus, E', for a reference temperature of 40°C. In principle, the loss moduli could be calculated from the E' data using the Kronig–Kramers relations.

The two master curves were obtained, according to the time–temperature correspondence (TTC) [34–37], by the horizontal shift along the log f axis of isothermal data obtained at different temperatures (between −0.9 and 80.4°C for PEc and between 17.9 and 94°C for PEs). Some authors claim that a vertical shift is also required for the construction of the master curves in HDPE [13,20] due to the fact that the relaxed and unrelaxed moduli are temperature dependent. However, those are found to be small (sometimes ±0.1 in the log E' scale [20]), which may be difficult to detect when one needs simultaneously to carry out the horizontal shift, i.e. the changes are made along two degrees of freedom. Therefore, in many cases (for example in Refs. [38,39]), the vertical shift is neglected. The use of the TCC principle will be discussed more in detail in Section 7.

Fig. 5 shows that, as expected, the storage modulus increases with increasing temperature and the inflexion on the two curves indicates that a relaxation process is involved in our frequency/temperature ranges. This was confirmed clearly by the existence of a maximum in the E'' and $\tan\delta$ plots. The position of these peaks in the temperature axis allows this relaxation to be attributed to the αI-process [12,13]. No peak was found at higher temperatures, i.e. the

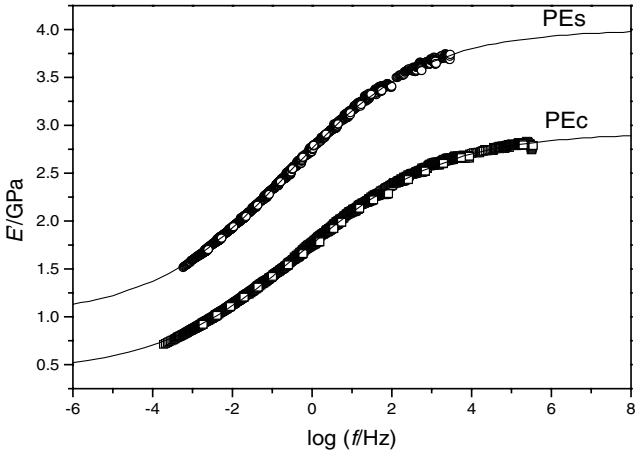

Fig. 5. Isothermal master curve for the storage modulus, E', in the α-relaxation region of HDPE. The reference temperature is 40°C. Squares are for PEc and circles are for PEs. The individual isothermal experiments were performed at different temperatures, from 0 to 95°C, where the frequency was scanned from 0.5 to 30 Hz.

Table 2
Cole–Cole parameters for the dynamic mechanical results of PEc and PEs at 40°C

	E_r (GPa)	E_u (GPa)	α_{CC}	τ_0 (s)
Pec	0.4	2.9	0.77	0.31
Pes	1.0	4.0	0.76	0.64

αII-process was not revealed in the data. It must be noted that in a number of papers the αII-process was also not seen in the results (for example Refs. [20,38,39]). As we shall discuss later, some αII character may be included in the unique α-peak observed. In order to facilitate the discussion, the relaxation observed in the dynamic results will be named, as reported frequently, simply as the α-process.

As commented before, 180° jumps of the chain stems in the crystallites are the dominant modes in the α-relaxation [12,13]. This process was observed clearly recently for the first time by nuclear magnetic resonance (NMR) [16]. The motion involves a translation of one CH_2-unit and a rotation such that the portion of the chain in the crystallites is in its energetically most favourable position in the lattice before and after the jump [40]. This process occurs with activation energies of 105 kJ mol^{-1}, which are similar to the corresponding values obtained by dielectric and mechanical experiments.

The α-process is dielectrically active due to the reorientation of carbonyl group defects in the chain [13]. However, the screw motions within the crystal structure just discussed could not account for mechanical relaxation by themselves because the chain flips occur between energetically equivalent states. The relaxation emerges from an additional shear of the amorphous regions that needs to occur in order to provide the chain transport through the lamellae. Hence, in the mechanical α-process, a relaxation mode in the crystallites and another located in the amorphous zones become combined. This composite nature complicates significantly the mechanisms associated with this process due to the occurrence of a large group of relaxational modes, assigned to processes occurring both in the crystalline phase and in the amorphous regions near the crystallites.

It was found [41] that the frequency-dependence behaviour of the α-process could be described adequately with the empirical Cole–Cole equation that was first derived to discuss dielectric results [42]:

$$E^*(\omega) = E_u + \frac{E_r - E_u}{1 + (i\omega\tau_0)^{1-\alpha_{CC}}} \quad (1)$$

where E_u and E_r are the unrelaxed and relaxed moduli, τ_0 is the average relaxation time, ω is the angular frequency ($\omega = 2\pi f$) and α_{CC} is a fitting parameter between 0 and 1 related to the width of the distribution of the relaxation times. For the particular case of $\alpha_{CC} = 0$ the system is described by a single relaxation time and could be modelled by a standard linear solid scheme (elastic spring in series with a Voigt–Kelvin unit) [22]. The real component of the Cole–Cole complex modulus is given by:

$$E'(\omega) = E_u + \frac{E_r - E_u}{2} \times \left\{1 - \frac{\sinh[(1-\alpha_{CC})X]}{\cosh[(1-\alpha_{CC})X] + \sin(\alpha_{CC}\pi/2)}\right\}, \quad (2)$$

$$X = \ln(\omega\tau_0)$$

Eq. (2) was used to fit the two data sets in Fig. 5 with E_u, E_r, τ_0 and α_{CC} as adjustable parameters. The solid lines correspond to the best fitting curves and the corresponding parameters are shown in Table 2.

The relaxation strength, given by $\Delta E' = E_u - E_r$, amounts to 2.5 and 3.0 GPa for PEc and PEs, respectively. Thus the occurrence of the α-relaxation leads to strong differences in the mechanical performance of PE. This fact strengthens the location of the deformation mode involved in the α-relaxation in the weak part of the polymer structure, i.e. in the amorphous region, which can be sheared easily. The high value of $\Delta E'$ for SCORIM-processed HDPE can be explained possibly by the higher crystallinity of the sample that implies a higher surface area of the crystalline phase and consequently a greater volume of amorphous region located near the lamellae that is involved in the α-relaxation.

The average relaxation times of the process at 40°C are in the range 0.3–0.7 s. The location of the α-relaxation in the temperature axis strongly depends on the lamellae thickness [2]. However, the results obtained are qualitatively consistent with other studies on HDPE that indicate a dispersion at ~50°C of the α-relaxation for frequencies around 1 Hz [13,21].

The α_{CC} values in Table 2 can be used to investigate the distribution of relaxation times. The corresponding probability density function of the relaxation times for

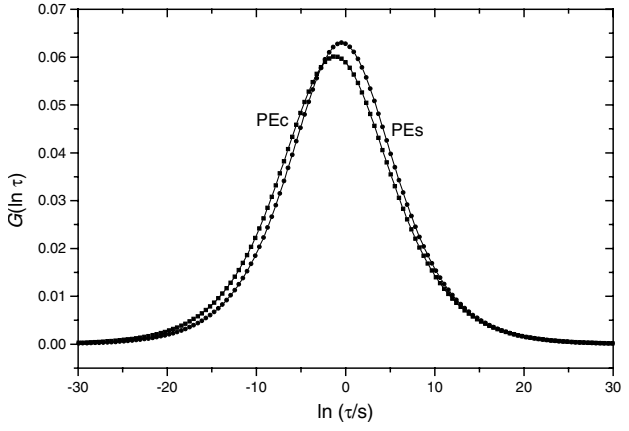

Fig. 6. Probability density function for the relaxation times involved in the α-relaxation in HDPE at 40°C. The curves were calculated from the Cole–Cole model. Squares correspond to PEc and circles to PEs samples.

Cole–Cole described systems is:

$$G(\ln \tau) = \frac{1}{2\pi} \frac{\sin(\pi\alpha)}{\cosh[(1-\alpha_{CC})\ln(\tau_0/\tau)] - \cos(\pi\alpha_{CC})} \quad (3)$$

The distribution curves are shown in Fig. 6 for the two processing methods at 40°C. The shape of the observed peaks should not depend on temperature because, as seen before, the time–temperature superposition should be valid for these systems. Obviously, the location of the peaks in the time/frequency axis depends on temperature and this effect can be predicted by inspection of the temperature-dependence of the shift factor.

The maxima of the two curves occur at $\tau = \tau_0$ values that are similar for both cases. Furthermore, the broadness of the peaks is pronounced but also very similar for PEc and PEs. It is interesting to note that the temperature location of the loss modulus at 1 Hz for ultra-high molecular weight PE fibres is similar to that of isotropic HDPE [43]

The broadness is related to the participation of the amorphous phase in the α-relaxation. In fact, different levels of entanglement and free-volume environment and the variety of segment lengths involved in the process lead to different relaxation times associated with the corresponding molecular motions. Given the similar amorphous phase of PEc and PEs, a similar broadness of the distribution of relaxation times should be expected. This is in fact observed, consistent with the same values of the Cole–Cole α_{CC} parameter observed for both materials (see Table 2). The value $\alpha_{CC} = 0.77$ from the dynamic results, is higher than that reported in Ref. [13] for compression-moulded HDPE ($\alpha_{CC} = 0.6$). The difference may arise from the injection moulding processing that creates complex stress fields within the cooling melt and gives rise to more complex and heterogeneous amorphous structures; this should lead to a broadening of the distribution of relaxation times assigned to the α-process.

The Cole–Cole α_{CC} parameter observed in dielectric results is in the range 0.2–0.3 [44], i.e. the distribution of relaxation times is much narrower than in mechanical results. This fact implies the strong contribution of the amorphous phase to the mechanical α-response. In the dielectric case, only the screw motion within the crystalline phase is sufficient in order to measure the α-relaxation process, provided that some dipolar groups exist in the PE chains. These molecular motions detected by dielectric measurements are more restricted in terms of the variety of molecular environments involved when compared with the mechanical-active ones.

Another hypothesis for the broad distribution of relaxation times of the mechanical α-relaxation is due to the existence of more than one mechanism (at least the αI and αII processes).

From comparison with NMR results [40] we can also argue for the contribution of the amorphous phase to the mechanical response in the α-relaxation. As commented before, the screw motion of the CH_2 groups along the crystalline chains observed by NMR are also intervening in the dielectric and mechanical α-relaxation. One can conclude this, for example, from the similarity of the activation energies. However, a difference of about four orders of magnitude is found between the rate of the elementary steps involved in the NMR experiments and the mechanical α-relaxation rate [21]. This indicates that, despite the same energy barriers involved in the process as observed by the two methods, the much slower mechanical relaxation reflects the shear component of the highly entangled amorphous phase.

6. Creep results

Creep is an important and powerful experimental method for the evaluation of physical properties of polymers, including viscoelastic behaviour and physical ageing. Moreover, creep is also a common phenomenon in engineering applications as it reflects the load-bearing capacity of end-products. Creep experiments were performed at different temperatures in PEc and PEs at a single stress of 0.1 MPa. A master curve was constructed for the engineering strain ε with the reference temperature $T_{ref} = 20$°C. The results are shown in Fig. 7.

As expected, the strain values are higher for PEc than for PEs throughout the entire time axis range investigated. The results also suggest a continuous increase of the strain in which no inflexion in the curves is observed. This difficulty of directly observing the α-relaxation of polyethylene from creep experiments has been reported several times (see for example Refs. [33,38,45,46]). It is interesting to note that for stress relaxation in HDPE studied with different drawing levels, a negative/positive curvature transition is detected [39] indicating the presence of the α-process.

The modelling of the creep results has been carried out by many researchers in the past three decades. A creep model consisting of two thermally activated Eyring-rate processes

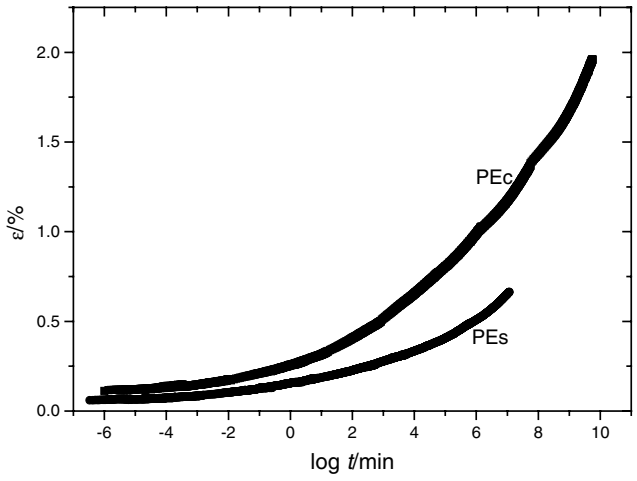

Fig. 7. Master curve of engineering strain ε for creep experiments at 20°C for HDPE. Squares are for PEc and circles are for PEs.

has been proposed by Ward and co-workers [1,38,46–50], particularly for ultra-high molecular weight polyethylene fibres. It has been seen that even in isotropic PE this model could describe the creep response [51] successfully. One process, dominant at high stress levels, has been attributed to the contribution of the crystalline phase. This process has also been regarded as the same mechanism as that of the mechanical α-relaxation. The other process, which dominates at low stress levels, has been assigned to the contribution from the amorphous network. The study of the applicability of this model would require results obtained under different temperatures and stresses.

7. Analysis of the temperature shift factor

The shift factor associated with the construction of the master curves for the dynamic experiments will now be examined. The corresponding Arrhenius plot of the dynamic data ($\log a_T$ vs $1/T$) is shown in Fig. 8. Several authors have described the results of the α-relaxation in PE, arguing that this process should be "thermally activated" and that the Glasstone–Laidler–Eyring model [30] assuming the existence of an activation energy E_a applies. Therefore, there should be a linear relationship between $\log a_T$ and $1/T$ that may be described by the Arrhenius equation:

$$a_{T/T_{ref}} = \exp\left[\frac{E_a}{R}\left(\frac{1}{T} - \frac{1}{T_{ref}}\right)\right] \quad (4)$$

The mean activation energy values, $\langle E_a \rangle$, obtained from the slope of the linear fitting of the dynamic data yield 190 and 160 kJ mol^{-1} for PEc and PEs, respectively. This information will be combined with the results of the Cole–Cole fittings of the master curves shown in Fig. 7. The procedure allows for the prediction of the isochronal viscoelastic response as a function of temperature for a fixed frequency.

In Fig. 9, the isochronal behaviour of PEc and PEs is shown in terms of the storage modulus in the temperature range 0–100°C for two frequencies 1 and 10 Hz (solid lines). The two curves were obtained using Eq. (2) where $\tau_0 = \tau_0' \exp(\langle E_a \rangle / RT)$, where T is now the independent variable and τ_0', the pre-exponential factor, was obtained by knowing one point of $\tau_0(T)$ for each material (the relaxation times, τ_0, of PEc and PEs at 40°C are, as seen in Table 2, 0.31 and 0.64 s, respectively). It must be remembered that all relevant parameters were obtained by fitting on the final master curves or during their construction (horizontal shifts).

Fig. 9 also shows the experimental storage moduli of PEc and PEs at 1 and 10 Hz in the same temperature region (symbols). Note that those points were taken from the original isothermal results. To collect this data, the iso-

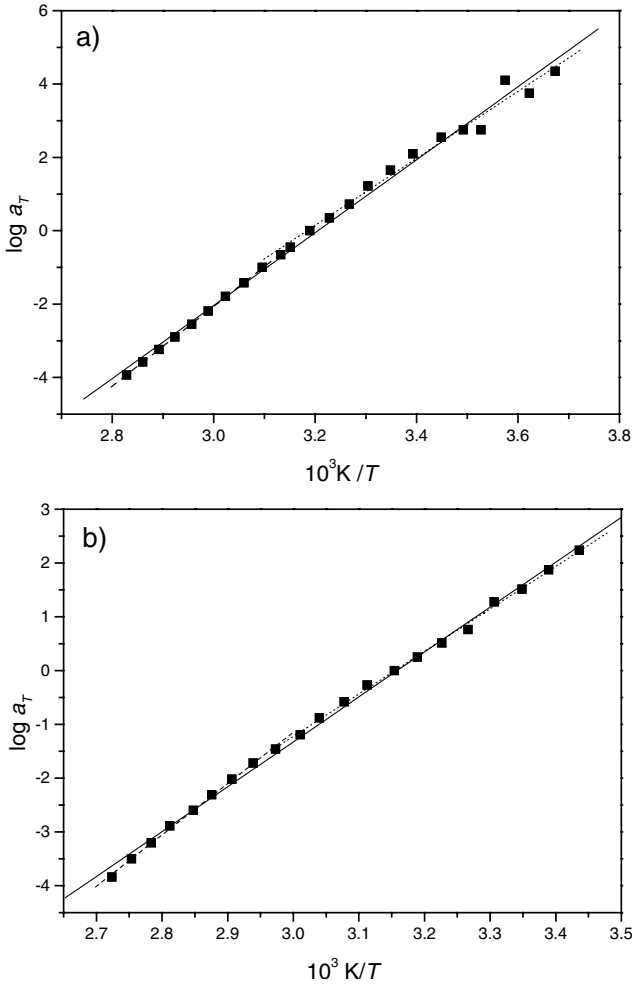

Fig. 8. Arrhenius plot of the logarithm temperature shift factor from dynamic mechanical E' results. Squares: experimental results; solid line: fitting considering all points; dashed line: fitting in the high-temperature region; dotted line: fitting in the low-temperature region. (a) Results for PEc. (b) Results for PEs.

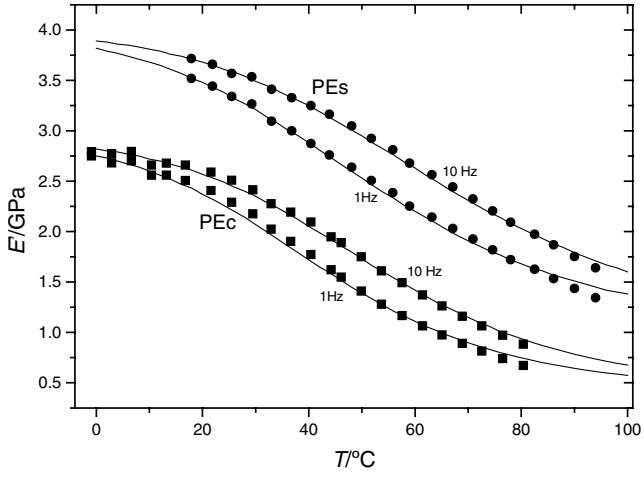

Fig. 9. Isochronal plot for the storage modulus at frequencies of 1 and 10 Hz in the α-relaxation region of HDPE. Expected results taken from a series of isothermal results (squares: PEc; circles: PEs). Solid lines: computing of the experimental results taking into account the fitting of the isothermal master curves with the Cole–Cole equation (results in Table 2) and assuming an Arrhenius equation for the temperature-dependence on the shift factor (mean activation energies in Table 3).

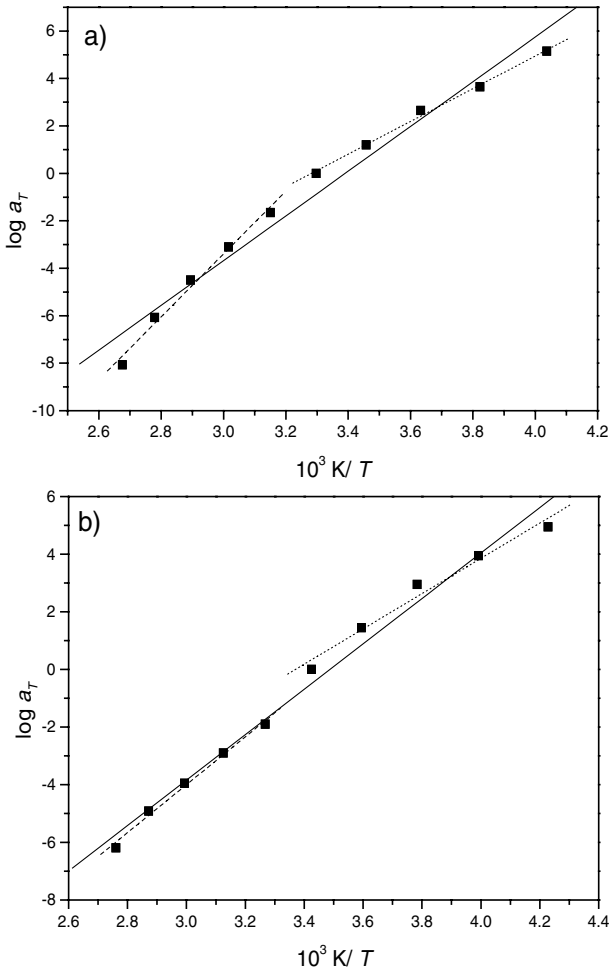

Fig. 10. Arrhenius plot of the logarithm temperature shift factor from the creep results. Squares: experimental results; solid line: fitting considering all points; dashed line: fitting in the high-temperature region; dotted line: fitting in the low-temperature region. (a) Results for PEc. (b) Results for PEs.

thermal E' vs. f results were inverted in order to have E' vs. T for each frequency. A very reasonable agreement is observed between the experimental data and the computed curves. The most pertinent conclusion of these results is the reinforcing of the thermorheological simplicity attribution of the α-relaxation.

A more careful inspection of Fig. 8 suggests a curvature in the plot, in the direction of an increase of the slope at higher temperatures. Some authors (see, for example, Ref. [20]) described this curvature in terms of the manifestation of the αI and αII processes, as described before, that have different activation energies. Fig. 10 shows the Arrhenius diagram for the creep results. In this case the curvature of the plots is even more pronounced. The activation energies obtained from creep are lower than those obtained from dynamic mechanical experiments, reflecting a dependence of E_a, a microscopic property, on the selected experimental technique. This seems to suggest that the Glasstone–Laidler–Eyring (Arrhenius-like) model may not be applicable to the materials we have investigated. However, a more detailed inspection still follows.

The activation energies on the low-temperature side (probably containing a higher αI character) and high-temperature side (richer in αII process) are presented in Table 3. Comparing the activation energies obtained in this work and those available in the literature, it was concluded that in our case the values are usually higher. In Ref. [20], PE films with very different draw ratios showed activation energies between 79 and 106 kJ mol^{-1} for the αI-process and 99–133 kJ mol^{-1} for the αII-process. Also for HDPE samples with distinct draw ratios, activation energies between 65 and 80 kJ mol^{-1} were reported [39]. A still larger interval was reported from dynamic studies on ultra-high strength PE fibre [52] where E_a varied from 88 to 210 kJ mol^{-1} for nearly linear chains and between 89 and 360 kJ mol^{-1} for highly branched chains. This scatter of the activation energy values could be related in part to variation of chemical structure and composition (molecular weight, branching, additives, etc.) and physical structure (general morphology, microstructure, orientation, crystalline degree, etc.) in polyethylene. However, quadrupling the value of 89 kJ mol^{-1} for highly branched chains shows that the physical significance of E_a in the studied system is doubtful at best. This reinforces the conclusion reached before on the basis of different E_a values obtained from different experiments. More work must be performed in order to clarify these controversial observations without ambiguity and we will still use E_a, at least, for comparative purposes.

Table 3 indicates that the inducing of orientation in HDPE decreases the slopes of the Arrhenius plot both in the low- and in the high-temperature regions. If these two temperature regions are assigned to the αI and αII processes, we may conclude that the processing affects both relaxation processes in a similar way. Matsuo et al. [20] also report a concomitant decrease of the activation energy of the αI and αII processes with increase of drawing, i.e. with increased anisotropy.

From the results presented in Table 3, it can be concluded that, despite the technique used, the activation energy is always higher for the injection-moulded material than for the SCORIM-processed specimens. This difference may reflect the orientation process of the crystalline phase undergone by the PEs sample during processing due to the higher

Table 3
Apparent activation energies (in kJ mol^{-1}) for PEc and PEs in dynamic and creep experiments. $\langle E_a \rangle$ is the mean activation energy calculated with all the points, αI and αII are for the calculus at the low- and the high-temperature sides

	PEc		PEs	
	Dynamic	Creep	Dynamic	Creep
$\langle E_a \rangle$	190	181	160	151
αI	175	132	151	117
αII	208	253	182	160

shear stresses cyclically applied to the melt during solidification. In the case of PEc this orientation process mainly occurred at the surface of the mould, whereas crystallisation throughout the core takes place under much more isotropic conditions. We note in this context that a decreasing of the activation energies was observed in PE films with increasing drawing levels, i.e. with increasing orientation within the crystalline phase [20].

From comparison between NMR, dielectric spectroscopy and dynamic mechanical studies it was concluded that molecular mobility within the crystalline phase should be required in order for the α-relaxation to be detected. Twist propagation of the CH_2 groups across the crystal has been modelled in atomistic detail [53]. The most efficient twist contains a series of about 12 CH_2 groups. This twist, once formed, can move through the surrounding lattice with little or no hindrance. There are energy barriers necessary to create a twist that could be related to the activation energy. Mechanical reactivity of PE in the α-relaxation region, as mentioned before, results from the advance of the chain and its effect on the amorphous interlayer.

The creation of a twist in the crystalline segments and the screw motion along the crystalline phase is then less hindered, on average, in PEs than in PEc due to higher crystalline order in the former case. New structures are formed during the continuous crystallisation under shear stresses, such as shish-kebab morphologies. In this case, high-order fibrillar crystalline structures are present allowing probably for a less hindered development of the molecular motions associated with the α-relaxation. The less ordered crystalline structures in the conventional injection-moulded samples, characterised basically of spherulitic lamellae, may be inferred from wide-angle X-ray diffraction experiments [8] and from the existence of a unique melting peak for PEc (maximum at 130.6°C), whereas a bimodal character is found for PEs [8] (maxima at 131.1 and 138.0°C). The existence of a higher-temperature melting peak in PEs suggests a more oriented fraction within the material.

Thus, if the activation energies represent anything at all in these systems, they presumably pertain to the crystalline structure. The amorphous phase located within the crystalline lamellae may be investigated by looking at distributions of relaxation times observed by mechanical spectroscopy techniques. The free-volume approach (to be discussed below) pertains to the material as a whole, although it can be split into crystal and amorphous contributions if materials with different degrees of crystallinity are investigated.

The slitting of the curvature of the Arrhenius plot into two different processes, presented here (or even three independent processes as suggested in Ref. [51]), may not be obvious, owing to the fact that the slope is continuously changing. However, in another study, the authors argued that the thermorheologically simple behaviour of the α-relaxation should be indicative of a single molecular process [38,54]. The fact that the Glasstone–Laidler–Eyring model leads to mutually exclusive interpretations may be one more proof of the model ambiguity when applied to this particular case.

The treatment of the α-process in HDPE as one unique process was also carried out by the group of Brostow [39]. He derived a general formula for the temperature-dependence of the shift factor using reduced volume concepts [55,56]:

$$\ln a_T = A + B/(v_r - 1) \tag{5}$$

where A and B are constants characteristic of a given viscoelastic material. The B parameter comes from the Doolittle viscosity η relation (η vs free volume) and could be close to $2.303 = \ln(10)$ for a variety of polymers. The reduced volume v_r is v/v^* where v is the specific volume and v^* is the characteristic volume, also called incompressible or hard-core volume. The free volume, v_f, can be calculated as $v_f = v - v^*$.

While Eq. (5) is fairly general, it requires an assumption on the temperature-dependence of v_r or v_f. The Hartmann equation of state, using reduced variables, has been shown to be applicable to a large number of materials including polymers [57,58]:

$$P_r v_r^5 = T_r^{3/2} - \ln v_r \qquad \text{where } P_r = P/P^*,\ T_r = T/T^* \tag{6}$$

where P and T are pressure and temperature and the r and * indexes stand for reduced and characteristic quantities, respectively. Since the experiments of the present study were conducted at atmospheric pressure, the term containing P_r in Eq. (6) is negligible, and we obtain,

$$v_r = \exp(T_r^{3/2}) \tag{7}$$

which can be substituted into Eq. (5).

Hartmann and Haque found $T^* = 1221$ K for HDPE [57], the value which shall be used for the PEc samples. Interaction energies in general depend on the interparticle distance. Since T^* represents the energetic situation in the system, this parameter should be necessarily different in PEc and PEs. As v^* corresponds to the situation when the entire free volume is "squeezed out"; the same values of v^* will be considered for PEc and PEs. Using Eq. (7) at room temperature (273 K), knowing that the density of PEc is 0.954 g cm^{-3}, the obtained value was $v^* = 0.932$ cm^3 g^{-1}, which is comparable to the values computed for other polyethylenes ($v^* = 0.9339$ cm^3 g^{-1} and $v^* = 0.9586$ cm^3 g^{-1} in Refs. [39,57], respectively). This value, applied to the PEs for which the density is equal to 0.962 g cm^{-3} yields, from Eq. (7), the specific temperature of $T^* = 1283$ K for this material. Thus, T^* is higher for the material with stronger interactions — in our case more orientation — as it should be. The same conclusions have been reached by Berry et al. [59] for their series of polymer liquid crystals.

Eqs. (5) and (7) were used to fit the $a_T(T)$ results. As the characteristic variables T^* and v^* were determined a priori,

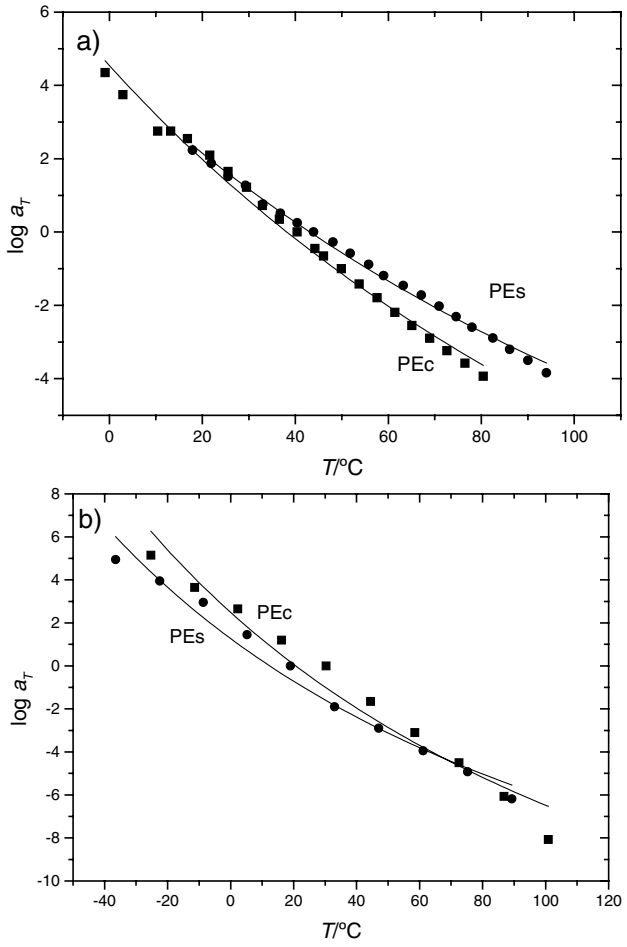

Fig. 11. Temperature-dependence of the shift factor for PEc (squares) and PEs (circles) in the α-relaxation region. The solid lines are the best fits using Eqs. (5) and (7) (the resulting parameters are shown in Table 4). (a) Results from dynamic mechanical experiments. (b) Results from creep experiments.

the only adjustable parameters were A and B. Fig. 11 shows the non-linear fittings of the dynamic (Fig. 11a) and creep results (Fig. 11b). Table 4 summarises the results of the best fittings. It is interesting to note that the parameter values obtained by the two techniques (dynamic mechanical analysis and creep) are similar for the same material obtained by a specific processing route. Thus, parameters A and B are material properties.

Despite the technique used, the B values are always higher in PEc than in PEs and an inverse trend is observed for the A values. These systematic tendencies reflect differences at the molecular level. There is an interesting issue here that should be addressed in future work. We note that in the polymer systems studied in Refs. [39,56] (polymer liquid crystals and HDPE) the authors always found $B > 2.303$, and often very close to the values obtained in this work. The values of A are found to increase with extended orientation. Similarly, for HDPE films with different draw ratios, λ, Boiko et al. found an increase of A with increasing λ [39]. The difference of the tendency for the A values in this work with that observed in such works [39,59] could be related to the relatively short extension of the orientation induced by the SCORIM procedure as compared with the consequences of the large draw ratios imposed on the samples or with the orientations achieved within liquid crystalline polymers.

Table 4
Results of fitting of $a_T(T)$ according to the Brostow model (combination of Eqs. (5) and (7))

	PEc		PEs	
	Dynamic	Creep	Dynamic	Creep
A	−45.4	−46.9	−38.7	−40.3
B	5.8	5.4	5.0	4.7
χ^2	0.056	0.81	0.014	0.37

8. Conclusions

The mechanical performance of HDPE can be enhanced by SCORIM processing due to the formation of highly oriented structures. The quasi-static mechanical testing of HDPE processed by SCORIM revealed an improvement of 59% in the flexural modulus when compared to the mechanical performance of conventionally injection moulding HDPE (PEc), that is consistent with the increase of tensile modulus reported in a previous work.

The effect of the orientation process on the viscoelastic properties has been studied in the α-relaxation region by means of dynamic mechanical tests and creep experiments. The obtained results support the following conclusions:

1. The α-relaxation response was found to be thermorheologically simple within the resolution of the results.
2. The dynamic results were described by the Cole–Cole equation. The width of the distribution of the relaxation times was found to be similar for both materials ($\alpha = 0.77$). The values of both the α coefficients and the relaxation strengths are explained by the intervention of conformational rearrangements within the amorphous phase during the α-relaxation. The amorphous phase near the crystallites is, thus, structurally similar in both materials (moulded under very distinct thermomechanical environments).
3. From the analysis of the temperature-dependence of the shift factor it was found that the mean activation energy of the α-process in PEs is lower than in PEc. Since this parameter reflects the energy barrier evolved in the twist motion of the polymer chains within the crystalline phase, it may be expected that this process is less hindered in PEs, possibly due to the presence of different lamellae organisations, such as shish-kebab structures.
4. The curvature found in the Arrhenius plots may be explained by the occurrence of two processes, well

described in the literature, but still controversial. Well-distinct activation energies values were obtained for these two possible mechanisms (150–170 and 180–210 kJ mol^{-1} for the αI and αII processes), respectively. The induction of orientation was found to decrease the activation energies of the two components in a similar way.

5. A parallel interpretation of the curvature of the Arrhenius lines was also considered, assuming a unique process. In this case, the α-process was described by a model proposed by Brostow (Eq. (5)), where the temperature-dependence of the reduced volume is given by Eq. (7). The relevant parameters of this model are found to be dependent on the processing route used (i.e. on the micro-structure) rather than on the technique used for the characterisation of the viscoelastic properties.

Acknowledgements

We thank Prof. W. Brostow, Dr B. Hartmann and Dr A. Goldman for valuable comments and suggestions on preparing this paper. One of us (R.A.S.) gratefully acknowledges financial support of Subprograma Ciência e Tecnologia do 2° Quadro Comunitário de Apoio, Ministério da Ciência e Tecnologia, Portugal.

References

[1] Cappacio G, Ward IM. Nature Phys Sci 1973;243:143.
[2] Ward IM, Wilding MA. J Polym Sci Polym Phys Ed 1984;22:561.
[3] Coates PD, Ward IM. Polymer 1979;20:1553.
[4] Gibson AG, Ward IM. J Polym Sci Polym Phys Ed 1978;16:2015.
[5] Hine PJ, Ward IM, Olley RH, Basset DC. J Mater Sci 1993;28:316.
[6] Kubát J, Månson JA. Polym Engng Sci 1983;23:869.
[7] Ogbonna CI, Kalay G, Allan PS, Bevis MJ. J Appl Polym Sci 1995;58:2131.
[8] Kalay G, Sousa RA, Reis RL, Cunha AM, Bevis MJ. J Appl Polym Sci 1999;73:2473.
[9] Allan PS, Bevis MJ. Plast Rubber Process Appl 1987;7:3.
[10] Kalay G, Ogbonna CI, Allan PS, Bevis MJ. Trans IChemE 1995;73A:788.
[11] Ogbonna CI. PhD thesis, Brunel University, UK, 1990.
[12] McCrum NG, Read BE, Williams G. Anelastic and dielectric effects in polymer solids. New York: Dover, 1991.
[13] Boyd RH. Polymer 1985;26:323 (see also p. 1123).
[14] Schmieder K, Wolf K. Kolloid Z 1953;134:149.
[15] Holzer B, Strobl GR. Acta Polym 1996;47:40.
[16] Hu W-G, Boeffel C, Schidt-Rohr K. Macromolecules 1999;32:1611.
[17] Flocke HA. Kolloid-Z Z Polym 1962;180:188.
[18] Nakayasu H, Markovitz H, Plazek DJ. Trans Soc Rheol 1961;5:261.
[19] McCrum NG, Morris EL. Proc R Soc (Lond) 1964;A281:258.
[20] Matsuo M, Sawatari C, Ohhata T. Macromolecules 1988;21:1317.
[21] Strobl G. The physics of polymers. Berlin: Springer, 1996.
[22] Ward IM, Hadley DW. An introduction to the mechanical properties of solid polymers. Chichester: Wiley, 1993.
[23] Suehiro S, Yamada T, Inagaki H, Kyu T, Nomura S, Kawai H. J Polym Sci Polym Phys Ed 1979;17:763.
[24] Suehiro S, Yamada T, Kyu T, Fujita K, Hashimoto T, Kawai H. Polym Engng Sci 1979;19:929.
[25] Suehiro S, Kyu T, Fujita K, Kawai H. Polym J 1979;11:331.
[26] Kawai H, Suehiro S, Kyu T, Shimomura A. Polym Engng Rev 1983;3:109.
[27] Takayanagi M. Med Fac Engng Kyushu Univ 1963;23:1.
[28] Iwayanagi S. Rep Prog Polym Phys (Jpn) 1962;5:131.
[29] Iwayanagi S. Prog Polym Phys (Jpn) 1962;V:135.
[30] Glasstone SK, Laidler KJ, Eyring H. The theory of rate processes. New York: McGraw-Hill, 1941.
[31] Keller A, Kolnaar H. In: Meijer H, editor. Flow induced orientation and structure formation, processing of polymers, Materials science and technology, vol. 18. 1997 (p. 191).
[32] Lai J, Bakker A. Scr Metall Mater 1993;28:1447.
[33] Lai J, Bakker A. Polymer 1995;36:93.
[34] Ferry JD. Viscoelastic properties of polymers. 3rd ed. New York: Wiley, 1980.
[35] Aklonis JJ, McKnight WJ. Introduction to polymer viscoelasticity. 2nd ed. New York: Wiley, 1983.
[36] Goldman YM. Prediction of the deformation properties of polymeric and composite materials. Washington, DC: American Chemical Society, 1994.
[37] Brostow W, Kubát M, Kubát MJ. In: Mark JE, editor. Physical properties of polymers handbook. Woodbury, NY: American Institute of Physics Press, 1996 (chap. 33).
[38] Govaert LE, Bastiaansen CWM, Leblans PJR. Polymer 1993;34:534.
[39] Boiko YM, Brostow W, Goldman AY, Ramamurthy AC. Polymer 1995;36:1383.
[40] Schmidt-Rohr K, Spiess HW. Macromolecules 1991;24:5288.
[41] Boyd RH. Macromolecules 1984;7:903.
[42] Cole RH, Cole KS. J Chem Phys 1941;9:341.
[43] Gibson AG, Davies GR, Ward IM. Polymer 1978;19:683.
[44] Aschcraft CR, Boyd RH. J Polym Sci Phys Ed 1976;14:2153.
[45] Duxbury J, Ward IM. J Mater Sci 1987;22:1215.
[46] Zhou H, Wilkes GL. Polymer 1998;39:3597.
[47] Wilding MA, Ward IM. Polymer 1978;19:969.
[48] Wilding MA, Ward IM. J Mater Sci 1984;19:629.
[49] Penning JP, Pras HE, Penning A. J Colloid Polym Sci 1994;272:664.
[50] Sengonul A, Wilding MA. Polymer 1995;36:4579.
[51] Bonner M, Duckett RA, Ward IM. J Mater Sci 1999;34:1885.
[52] Ohta Y, Yasuda H. J Polym Sci Phys Ed 1994;32:2241.
[53] Mansfield M, Boyd RH. J Polym Sci Phys Ed 1978;16:1227.
[54] Govaert LE, Lemstra PJ. Colloid Polym Sci 1992;270:455.
[55] Brostow W. Mater Chem Phys 1985;13:47.
[56] Brostow W, D'Sousa NA, Kubát J, Maksimov R. J Chem Phys 1999;110:9706.
[57] Hartmann B, Haque MA. J Appl Phys 1985;58:2831.
[58] Hartmann B, Haque MA. J Appl Polym Sci 1985;30:1553.
[59] Berry JM, Brostow W, Hess M, Jacobs EG. Polymer 1998;39:4081.